Supplementary Material for Real-time 3D Visualization of Radiance Fields on Light Field Displays

JONGHYUN KIM*, NVIDIA, USA
CHENG SUN*, NVIDIA, USA
MICHAEL STENGEL*, NVIDIA, USA
MATTHEW CHAN, NVIDIA, USA
ANDREW RUSSELL, NVIDIA, USA
JAEHYUN JUNG, NVIDIA, USA
WIL BRAITHWAITE, NVIDIA, USA
DAVID LUEBKE, NVIDIA, USA
SHALINI DE MELLO, NVIDIA, USA

ACM Reference Format:
Jonghyun Kim, Cheng Sun, Michael Stengel, Matthew Chan, Andrew Russell, Jaehyun Jung, Wil Braithwaite, David Luebke, and Shalini De Mello. 2026. Supplementary Material for Real-time 3D Visualization of Radiance Fields on Light Field Displays. *Proc. ACM Comput. Graph. Interact. Tech.* 9, 4, Article 56 (July 2026), 17 pages. https://doi.org/10.1145/3820023

A Additional results

References

Jonathan T Barron, Ben Mildenhall, Dor Verbin, Pratul P Srinivasan, and Peter Hedman. 2022. Mip-nerf 360: Unbounded anti-aliased neural radiance fields. In *Proceedings of the IEEE/CVF conference on computer vision and pattern recognition*. 5470–5479.

*contributed equally to this research

Authors' Contact Information: Jonghyun Kim, NVIDIA, Santa Clara, CA, USA, jonghyunk@nvidia.com; Cheng Sun, NVIDIA, Santa Clara, CA, USA, chengs@nvidia.com; Michael Stengel, NVIDIA, Santa Clara, CA, USA, mstengel@nvidia.com; Matthew Chan, NVIDIA, Santa Clara, CA, USA, matchan@nvidia.com; Andrew Russell, NVIDIA, Santa Clara, CA, USA, arussell@nvidia.com; Jaehyun Jung, NVIDIA, Santa Clara, CA, USA, jaehyunj@nvidia.com; Wil Braithwaite, NVIDIA, Santa Clara, CA, USA, wbraithwaite@nvidia.com; David Luebke, NVIDIA, Santa Clara, CA, USA, dluebke@nvidia.com; Shalini De Mello, NVIDIA, Santa Clara, CA, USA, shalinig@nvidia.com.

ACM 2577-6193/2026/7-ART56
https://doi.org/10.1145/3820023

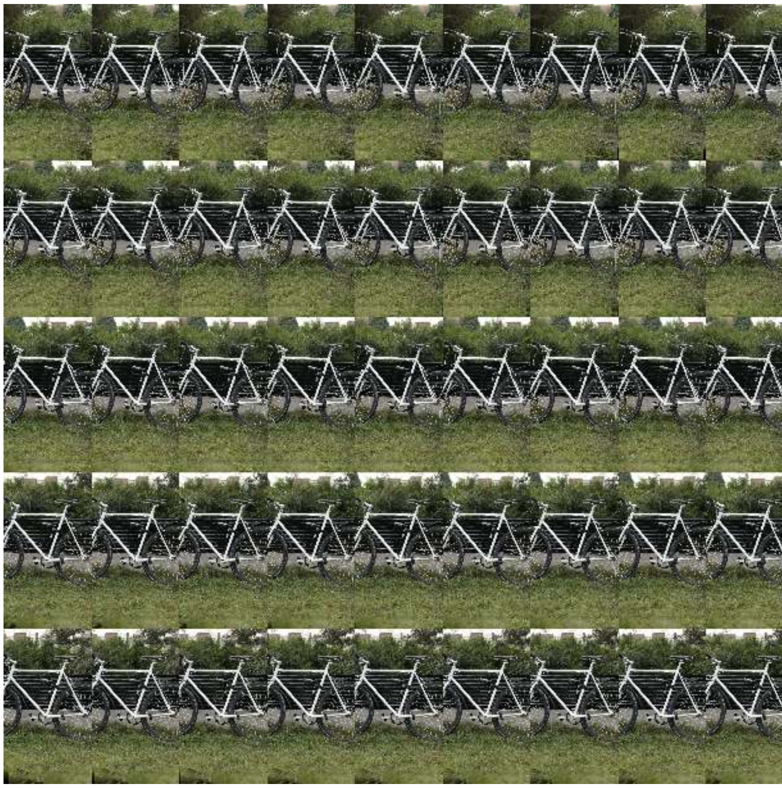

Fig. S1. Full 45-view light field quilt for Bicycle scene from the MipNeRF-360 dataset [Barron et al. 2022] rendered using G2LF algorithm for Looking Glass Go display (N_x = 512, N_y = 910, N_{chunk}=512).

Fig. S2. Captured results of the Bicycle scene from the MipNeRF-360 dataset [Barron et al. 2022] on a Looking Glass Go display for multiple algorithm variants. Each row corresponds to a different rendering method, and each column shows a captured viewpoint sampled across the display's horizontal viewing range. Although the rendering quality varies across methods, all variants preserve consistent view-dependent appearance and coherent 3D structure across viewpoints, confirming correct light-field reconstruction on the real display. In practice, artifacts visible in individual rendered views are less noticeable during actual viewing, as multiple views perceptually blend within the viewer's pupil.

Fig. S3. Evaluation on the rendered COUNTER scene from the MipNeRF-360 dataset [Barron et al. 2022]. (Top) Visual comparisons between the ground truth, the baseline models, and our proposed methods. (Bottom) Rendered light field quilt views across horizontal viewpoints for different algorithms. Our methods preserve consistent multi-view appearance while trading off rendering quality and speed. The numbers appended to G2LF and V2LF denote the N_{chunk}.

Fig. S4. Full 45-view light field quilt for Counter scene from the MipNeRF-360 dataset [Barron et al. 2022] rendered using G2LF algorithm for Looking Glass Go display (N_x = 512, N_y = 910, N_{chunk}=512).

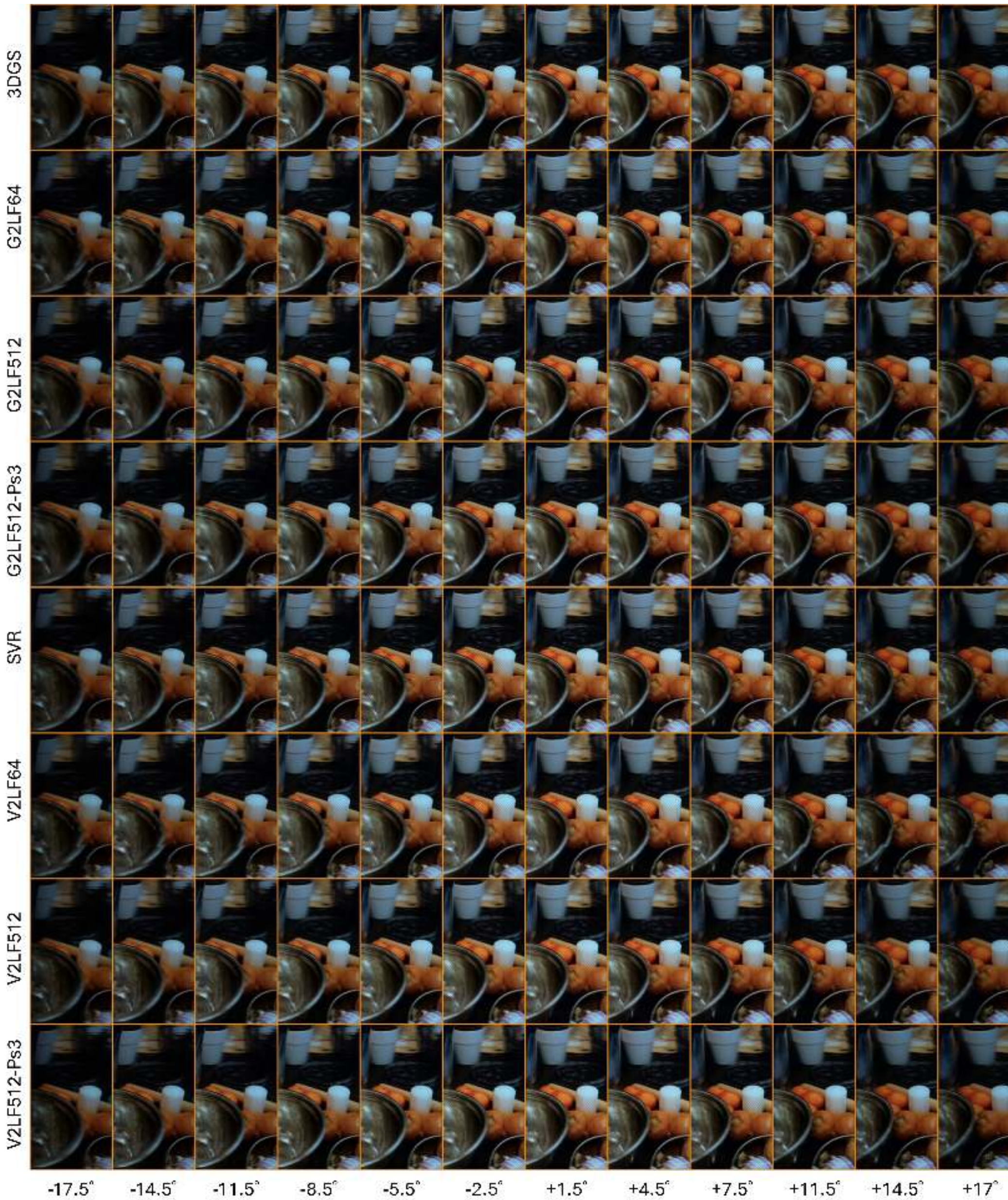

Fig. S5. Captured results of the Counter scene from the MipNeRF-360 dataset [Barron et al. 2022] on a Looking Glass Go display for multiple algorithm variants. Each row corresponds to a different rendering method, and each column shows a captured viewpoint sampled across the display's horizontal viewing range. Although rendering quality varies across methods, all variants preserve consistent multi-view appearance and coherent 3D structure across viewpoints. Artifacts visible in individual rendered views are less noticeable during actual viewing, as multiple views perceptually blend within the viewer's pupil.

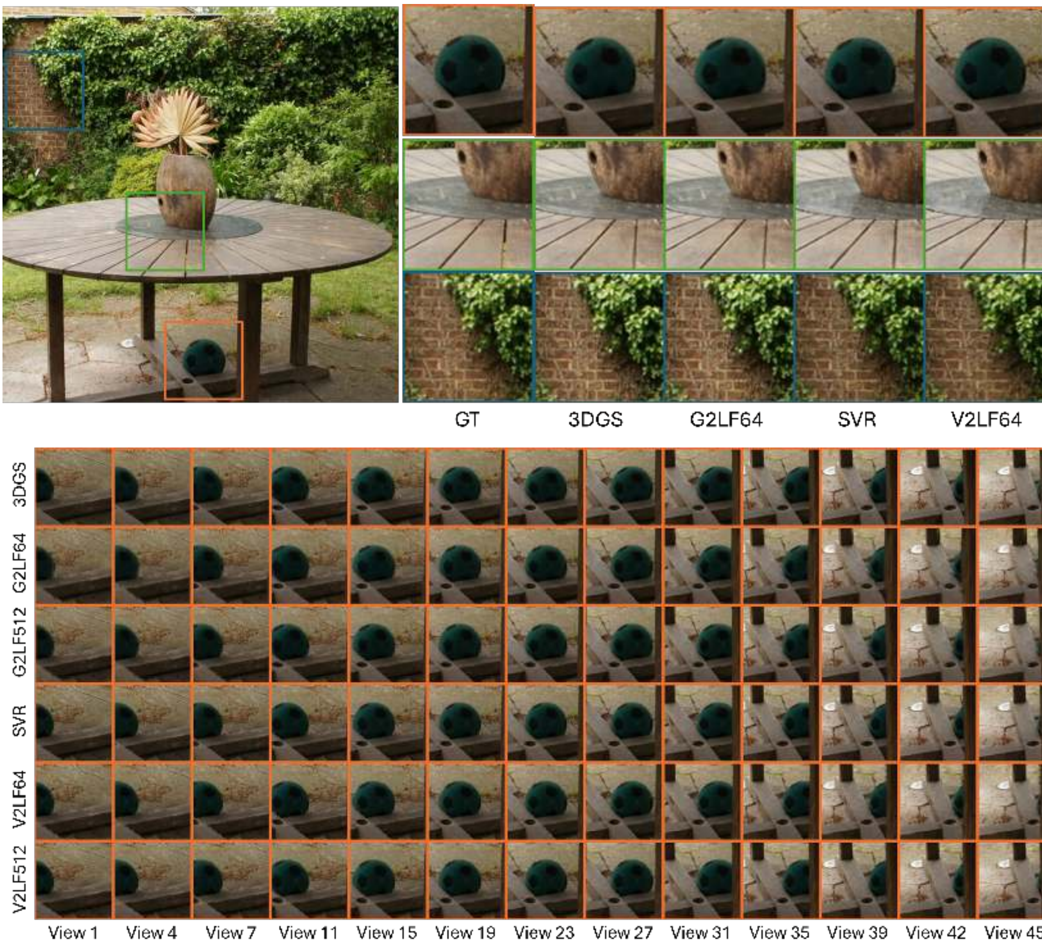

Fig. S6. Evaluation on the rendered GARDEN scene from the MipNeRF-360 dataset [Barron et al. 2022]. (Top) Visual comparisons between the ground truth, the baseline models, and our proposed methods. (Bottom) Rendered light field quilt views across horizontal viewpoints for different algorithms. Our methods preserve consistent multi-view appearance while trading off rendering quality and speed. The numbers appended to G2LF and V2LF denote the N_{chunk}.

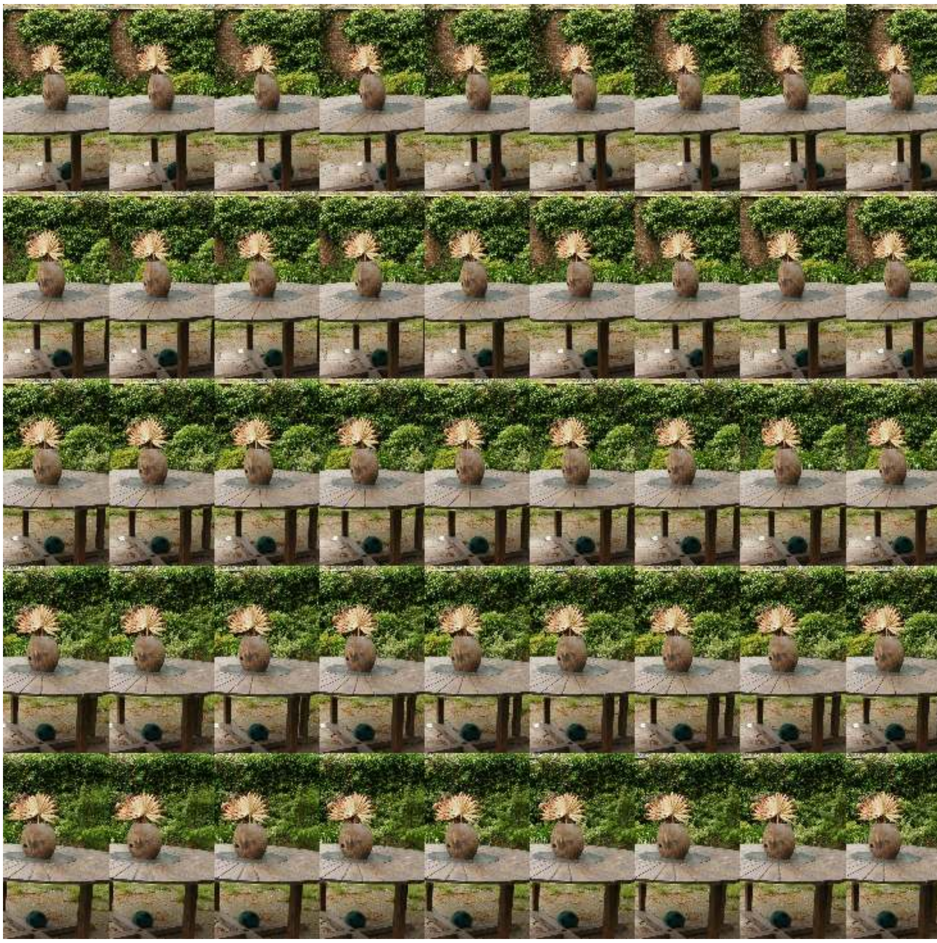

Fig. S7. Full 45-view light field quilt for GARDEN scene from the MipNeRF-360 dataset [Barron et al. 2022] rendered using G2LF algorithm for Looking Glass Go display (N_x = 512, N_y = 910, N_{chunk}=512).

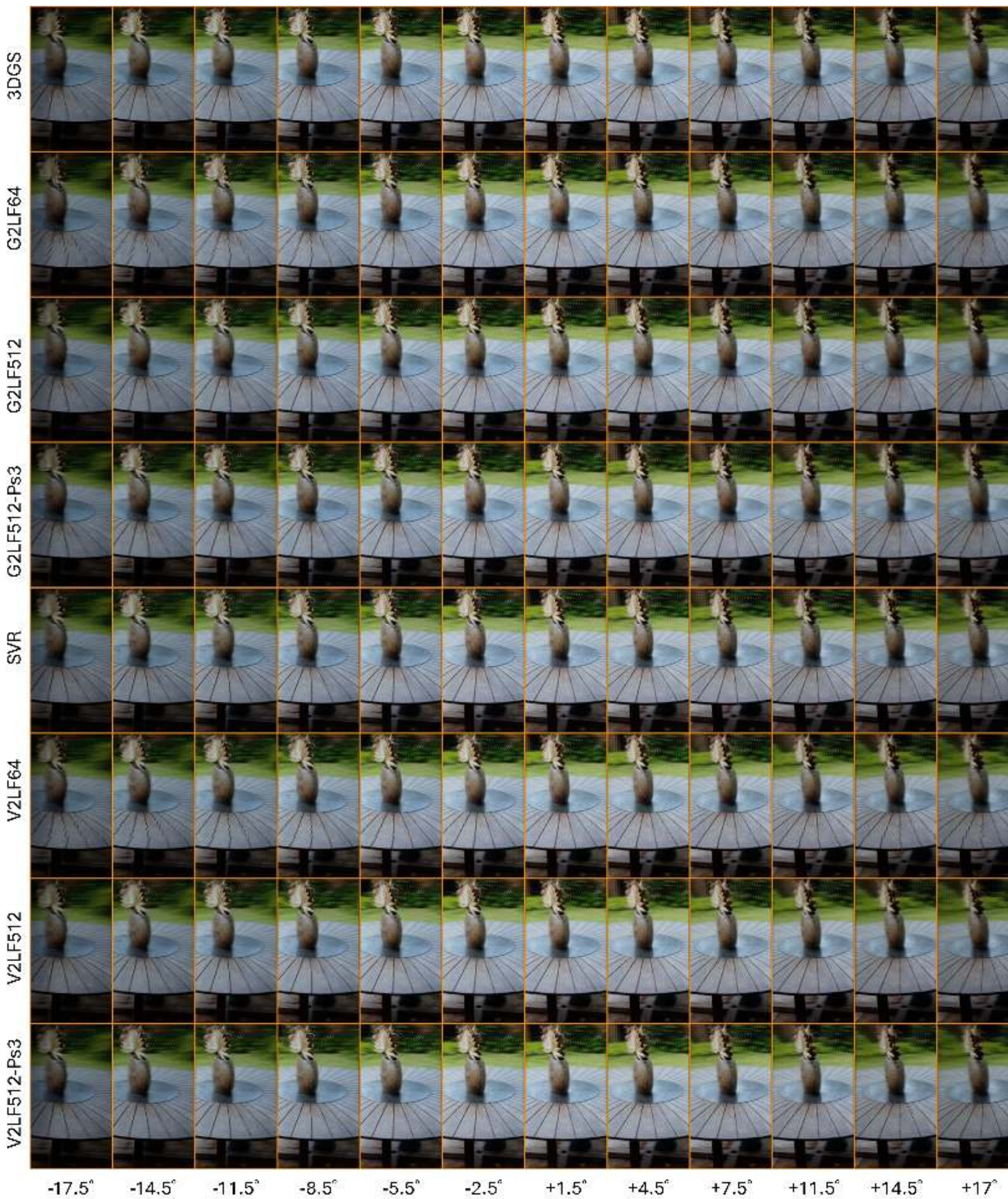

Fig. S8. Captured results of the GARDEN scene from the MipNeRF-360 dataset [Barron et al. 2022] on a Looking Glass Go display for multiple algorithm variants. Each row corresponds to a different rendering method, and each column shows a captured viewpoint sampled across the display's horizontal viewing range. Although rendering quality varies across methods, all variants preserve consistent multi-view appearance and coherent 3D structure across viewpoints. Artifacts visible in individual rendered views are less noticeable during actual viewing, as multiple views perceptually blend within the viewer's pupil.

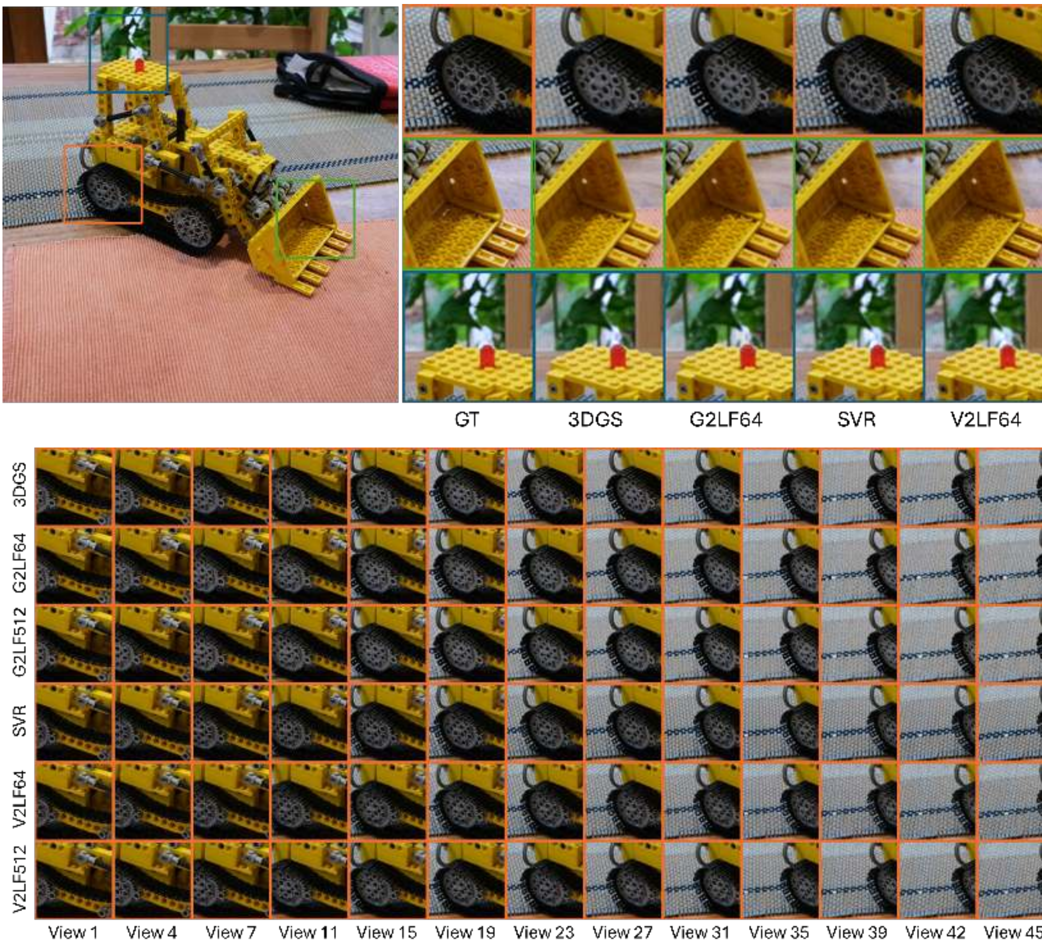

Fig. S9. Evaluation on the rendered Kitchen scene from the MipNeRF-360 dataset [Barron et al. 2022]. (Top) Visual comparisons between the ground truth, the baseline models, and our proposed methods. (Bottom) Rendered light field quilt views across horizontal viewpoints for different algorithms. Our methods preserve consistent multi-view appearance while trading off rendering quality and speed. The numbers appended to G2LF and V2LF denote the N_{chunk}.

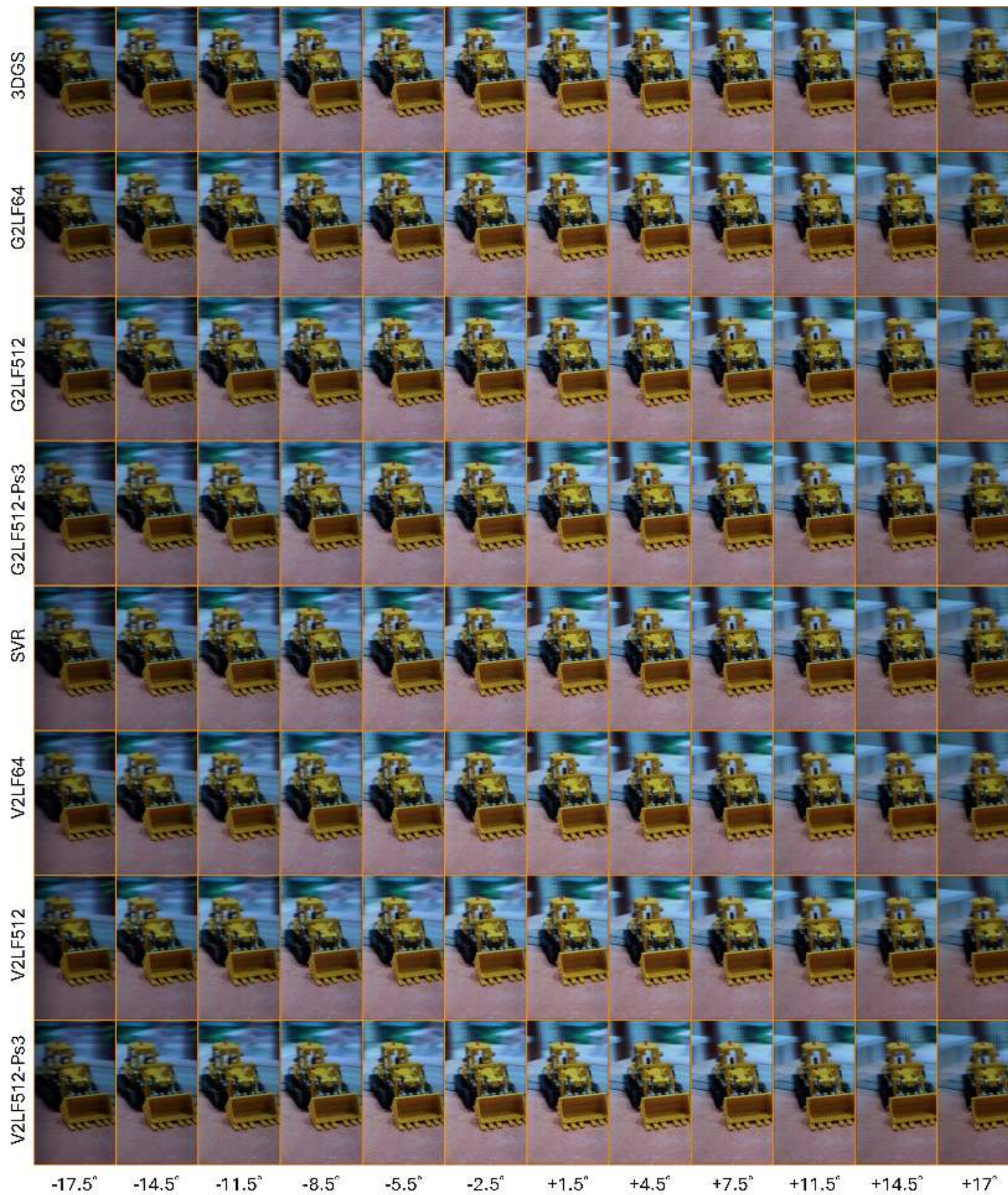

Fig. S10. Captured results of the Kitchen scene from the MipNeRF-360 dataset [Barron et al. 2022] on a Looking Glass Go display for multiple algorithm variants. Each row corresponds to a different rendering method, and each column shows a captured viewpoint sampled across the display's horizontal viewing range. Although rendering quality varies across methods, all variants preserve consistent multi-view appearance and coherent 3D structure across viewpoints. Artifacts visible in individual rendered views are less noticeable during actual viewing, as multiple views perceptually blend within the viewer's pupil.

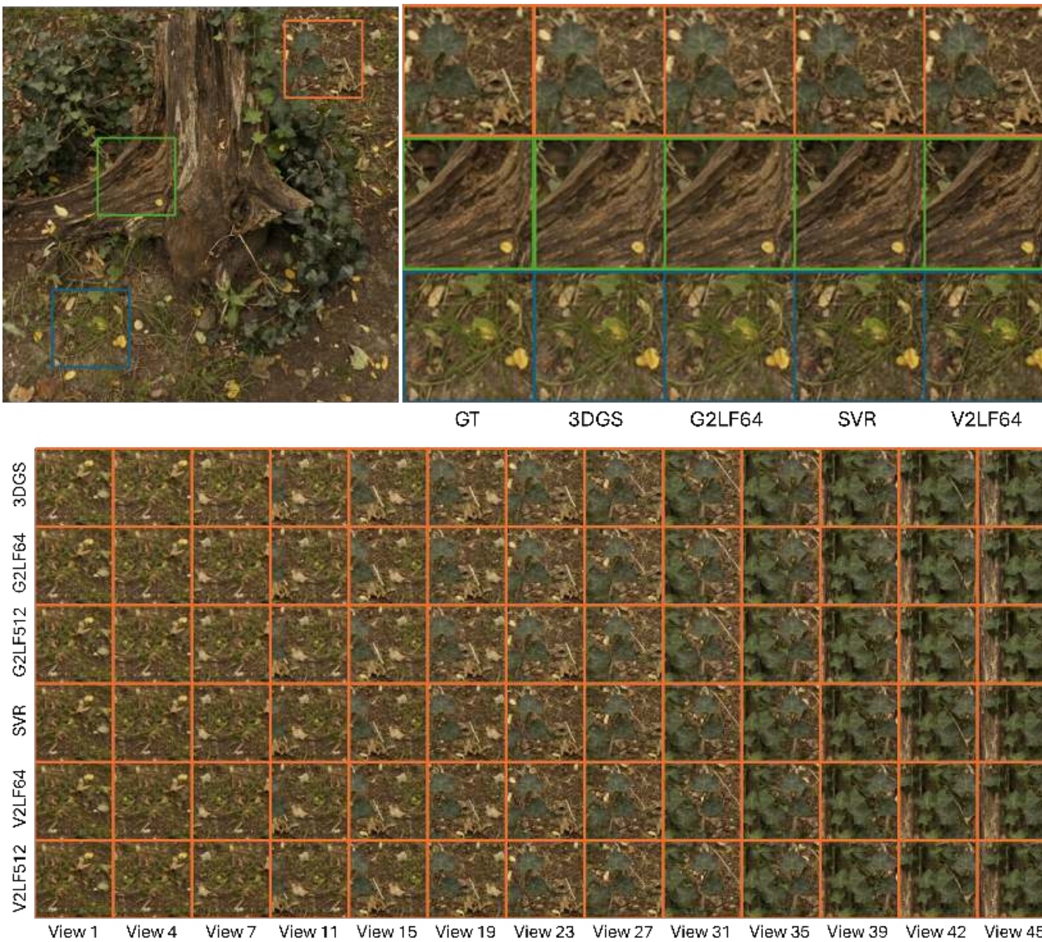

Fig. S11. Evaluation on the rendered Stump scene from the MipNeRF-360 dataset [Barron et al. 2022]. (Top) Visual comparisons between the ground truth, the baseline models, and our proposed methods. (Bottom) Rendered light field quilt views across horizontal viewpoints for different algorithms. Our methods preserve consistent multi-view appearance while trading off rendering quality and speed. The numbers appended to G2LF and V2LF denote the N_{chunk}.

Fig. S12. Full 45-view light field quilt for Stump scene from the MipNeRF-360 dataset [Barron et al. 2022] rendered using G2LF algorithm for Looking Glass Go display (N_x = 512, N_y = 910, N_{chunk}=512).

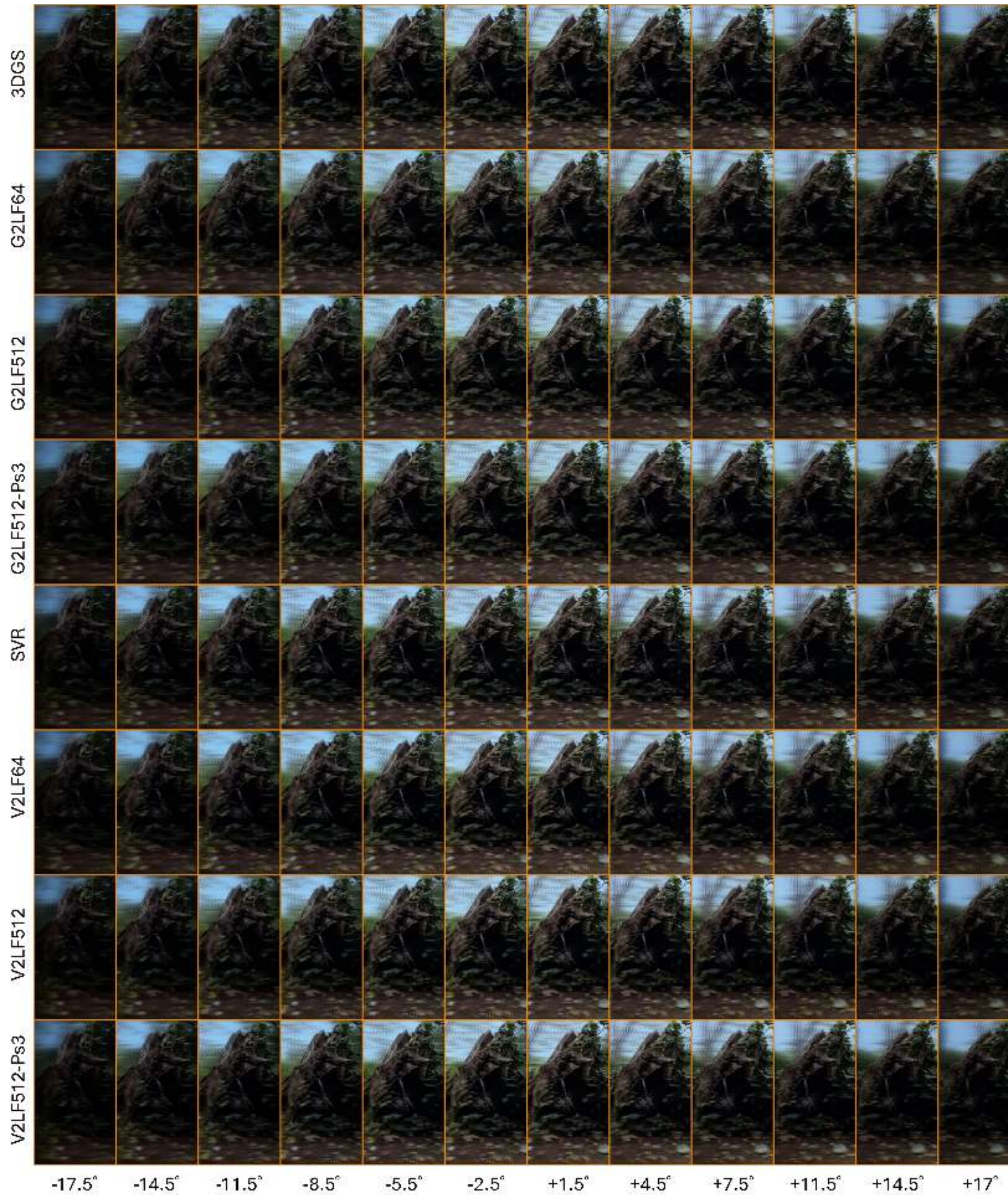

Fig. S13. Captured results of the Stump scene from the MipNeRF-360 dataset [Barron et al. 2022] on a Looking Glass Go display for multiple algorithm variants. Each row corresponds to a different rendering method, and each column shows a captured viewpoint sampled across the display's horizontal viewing range. Although rendering quality varies across methods, all variants preserve consistent multi-view appearance and coherent 3D structure across viewpoints. Artifacts visible in individual rendered views are less noticeable during actual viewing, as multiple views perceptually blend within the viewer's pupil.

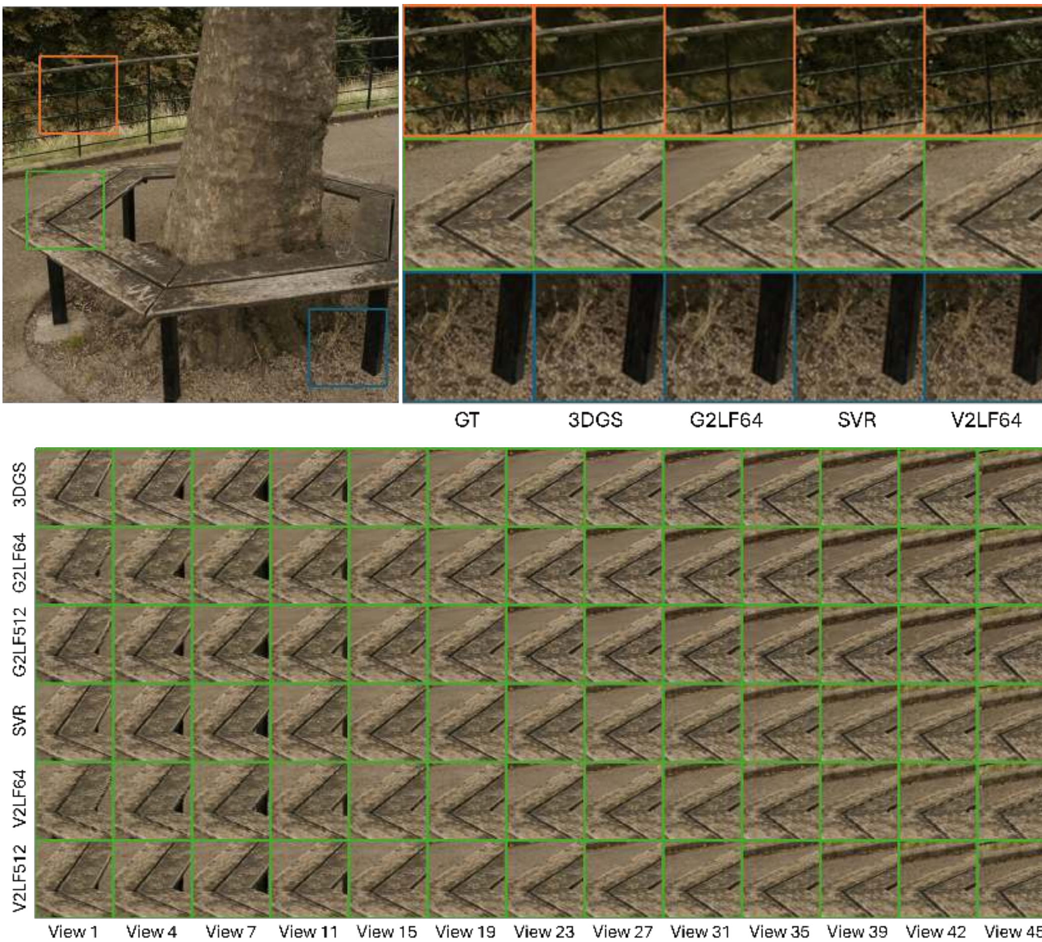

Fig. S14. Evaluation on the rendered TREEHILL scene from the MipNeRF-360 dataset [Barron et al. 2022]. (Top) Visual comparisons between the ground truth, the baseline models, and our proposed methods. (Bottom) Rendered light field quilt views across horizontal viewpoints for different algorithms. Our methods preserve consistent multi-view appearance while trading off rendering quality and speed. The numbers appended to G2LF and V2LF denote the N_{chunk}.

Fig. S15. Full 45-view light field quilt for Treehill scene from the MipNeRF-360 dataset [Barron et al. 2022] rendered using G2LF algorithm for Looking Glass Go display (N_x = 512, N_y = 910, N_{chunk}=512).

Fig. S16. Captured results of the Treehill scene from the MipNeRF-360 dataset [Barron et al. 2022] on a Looking Glass Go display for multiple algorithm variants. Each row corresponds to a different rendering method, and each column shows a captured viewpoint sampled across the display's horizontal viewing range. Although rendering quality varies across methods, all variants preserve consistent multi-view appearance and coherent 3D structure across viewpoints. Artifacts visible in individual rendered views are less noticeable during actual viewing, as multiple views perceptually blend within the viewer's pupil.